Electronic Supplementary Material (ESI) for Journal of Materials Chemistry A.

Supplementary Information

Ultrathin Cadmium Sulfide Nanosheets for Visible-Light Photocatalytic Hydrogen Production

Ya-Meng Xie, Xiao-Hua Liu, Rui Zhang, Hui Liu, Jing Mao, Cun-Ku Dong*, Xi-Wen Du *

Contents

1. Supplementary Methods

Chemicals. All chemicals were analytical grade and were used as received without further purification.

Synthesis of sulfide/metal/sulfide sandwich NSs. Sandwich NSs were synthesized in a two-temperature tube furnace by a thermal evaporation process. In a typical experiment, 0.15g Cd powder (99.5%) was added into a quartz boat. Then the quartz boat and FTO substrate were put in the middle of the high-temperature region (at 290 ℃) and low-temperature region (at to 200 ℃), respectively. The reaction lasted for 4 h at a pressure of 4.05 Torr with a continuous flow of mixed gas of 80% N_2 and 20% SO_2.

Synthesis of 1 nm NSs. 1 nm NSs was obtained by etching the as-prepared sandwich NSs with diluted acetic acid. The sandwich NSs was scraped off from the FTO substrate and then added into the aqueous solution of acetic acid (10 vol. %), and etched at room temperature for 7 days. Then the dispersion was centrifuged at 18000 rpm, washed repeatedly with ethanol and deionized water and freeze-dried to obtain the 1 nm NSs.

Synthesis of 5 nm NSs. The 5 nm NSs were synthesized by sulfuring sulfide/metal/sulfide sandwich NSs with sublimed sulfur. at 260℃ for 30 minutes. Nitrogen was used as carrier gas, and the flow rate was set as 100 sccm.

Synthesis of 15 nm NSs. The 15 nm NSs were synthesized by a thermal evaporation process reported in our previous work[1].

Material Characterization. The as-prepared materials were examined using X-ray

diffraction (XRD, Bruker-D8 advanced diffractometer with Cu Kα radiation), scanning electron microscopy (SEM, Hitachi S-4800), transmission electron microscopy (TEM, JEOL-2100F system equipped with EDAX Genesis XM2). For the preparation of TEM samples, the products were ultrasonically dispersed in ethanol, and the solution was dropped on a Cu grid coated with a holey carbon film and dried with air. STEM images were performed using a JEOL ARM200F microscope with STEM aberration corrector operated at 200 kV. The convergent semi-angle and collection angle were 21.5 and 200 mrad, respectively. The aberration coefficient used was equal to 1 μm. Atomic force microscopy (AFM) analysis was performed in air with a Multimode 8 Nanoscope (Veeco Instruments. Inductively coupled plasma mass spectrometer (ICP-MS) analysis was collected on Agilent 7700X. X-ray photoelectron spectroscopy (XPS) analysis was collected on a k-alpha Thermo fisher spectrometer (ThermoFisher Scientific). Prior to manipulation, all the VB spectra were background subtracted and normalized to a common intensity. The UV- visible diffuse reflectance spectra (DRS) were obtained using a UV-vis spectrophotometer (Hitachi, U-4100).

Measurements of photocatalytic hydrogen production. The measurements of photocatalytic H_2 production were carried out in a gas-closed system with a 100mL Pyrex flask (openings sealed with silicone rubber septum) at room temperature and ambient pressure. Before the experiment, all glassware was rinsed carefully with deionized water. A 300 W xenon lamp with an ultraviolet-cutoff filter (420 nm) was utilized as a visible-light source to trigger the photocatalytic reaction. The light intensity on the flask was about 100 $mW \bullet cm^{-2}$ (AM 1.5G). In a typical photocatalytic

experiment, the photocatalyst powder was suspended by constant stirring in 40 ml of 0.25 M Na_2S and 0.35 M Na_2SO_3 solution. The content of NSs samples was measured by ICP-MS. The average content of 1 nm, 5 nm and 15 nm NSs samples were determined as 1.47 μg, 0.88 mg and 0.84 mg, respectively. Before irradiation, the suspension was purged with argon for 0.5 h to remove dissolved air and keep the reaction system under anaerobic conditions. In the stability of hydrogen evolution experiment, no successive cooling water was added. After continuous photocatalytic hydrogen production test per hour, the suspension was purged with argon for 0.5 h to remove air and play a cooling role. Next, 0.2 mL gas was intermittently sampled through the septum, and H_2 content was analysed by gas chromatograph (GC-2014C, TCD, Ar as a carrier gas and 5 Å molecular sieve column).

Measurement of apparent and internal quantum efficiencies. For monochromatic light sources (λ = 420 nm), the accurate illumination power for a certain area of the reaction mixture (1 cm^2) was measured using a digital photodiode power meter (Newport, model 91150V). Photocatalytic hydrogen evolution set-up and sample dosage were the same as the measurements of photocatalytic hydrogen production. The system was then sealed and deoxygenated with argon for 30 min. Under constant stirring, the solution was irradiated at the same place and area as applied for power measurements above. The number of absorbed photons was calculated from the illumination power and the absorbance of solution from the reaction solution, while the molar amount of H_2 was quantitatively analyzed by GC. Based on the average of four experiments on 1 nm NSs, the illumination power (P) was determined as 5

mW/cm^2, the light transmittance (T%) of the reaction solution in 420 nm was 92.55 ± 0.01%, and hydrogen evolution over 1 h was 1.309 × 10^{-6} mol. Consequently, the internal quantum efficiency was calculated as follows[2]:

Amount of hydrogen molecules generated per second:

$$k_{H_2} = \frac{n_{H_2}}{t} = \frac{1.309 \times 10^{-6} mol \times 6.02 \times 10^{23}}{3600s} = 2.189 \times 10^{14}\ s^{-1}$$

Amount of incident photons per second:

$$q_{\text{incident photons}} = \frac{P\lambda}{hc} = \frac{5 \times 10^{-3} W \times 420nm}{6{,}626 \times 10^{-34}\ J \cdot s \times 3.0 \times 10^{8} m\ s^{-1}} = 1.056 \times 10^{16}\ s^{-1}$$

Amount of absorbed photons per second:

$$q_{\text{absorbed photons}} = q_{\text{incident photons}} \times (1 - T\%) = 1.056 \times 10^{16} s^{-1} \times (1 - 92.55\%) = 7.867 \times 10^{14} s^{-1}$$

Apparent quantum efficiency (AQY):

$$AQY = \frac{2k_{H_2}}{q_{\text{incident photons}}} \times 100\% = \frac{2 \times 2.189 \times 10^{14} s^{-1}}{1.056 \times 10^{16} s^{-1}} \times 100\% = 4.15\%$$

Internal quantum efficiency (IQY):

$$IQY = \frac{2k_{H_2}}{q_{\text{absorbed photons}}} \times 100\% = \frac{2 \times 2.189 \times 10^{14} s^{-1}}{7.867 \times 10^{14} s^{-1}} \times 100\% = 55.65\%$$

Accordingly, we also determined AQY/IQY of 5 nm NSs and 15 nm NSs.

DFT calculations. Density functional theory (DFT) calculations were performed based on structural parameters determined by XAENS, with the plane-wave basis code Vienna Ab initio simulation package (VASP). A plane-wave cutoff of 450 eV was used, and 5×5×5, 5×5×1 Monkhorst–Pack k-point grid were adopted for calculations on the inner and surface of 1 nm NSs, respectively. The atomic positions are allowed to relax until the energy and force are less than 10^{-5} eV/atom and 10^{-6}

eV/atom, respectively. Considering the calculation accuracy, the slab model with periodic boundary conditions was used to construct different CdS surface structure. The surface structure was built by Materials Studio software, and each crystal surface structure includes 5 original layers and the vacuum layer is set to 20 Å.

2. Supplementary Figures

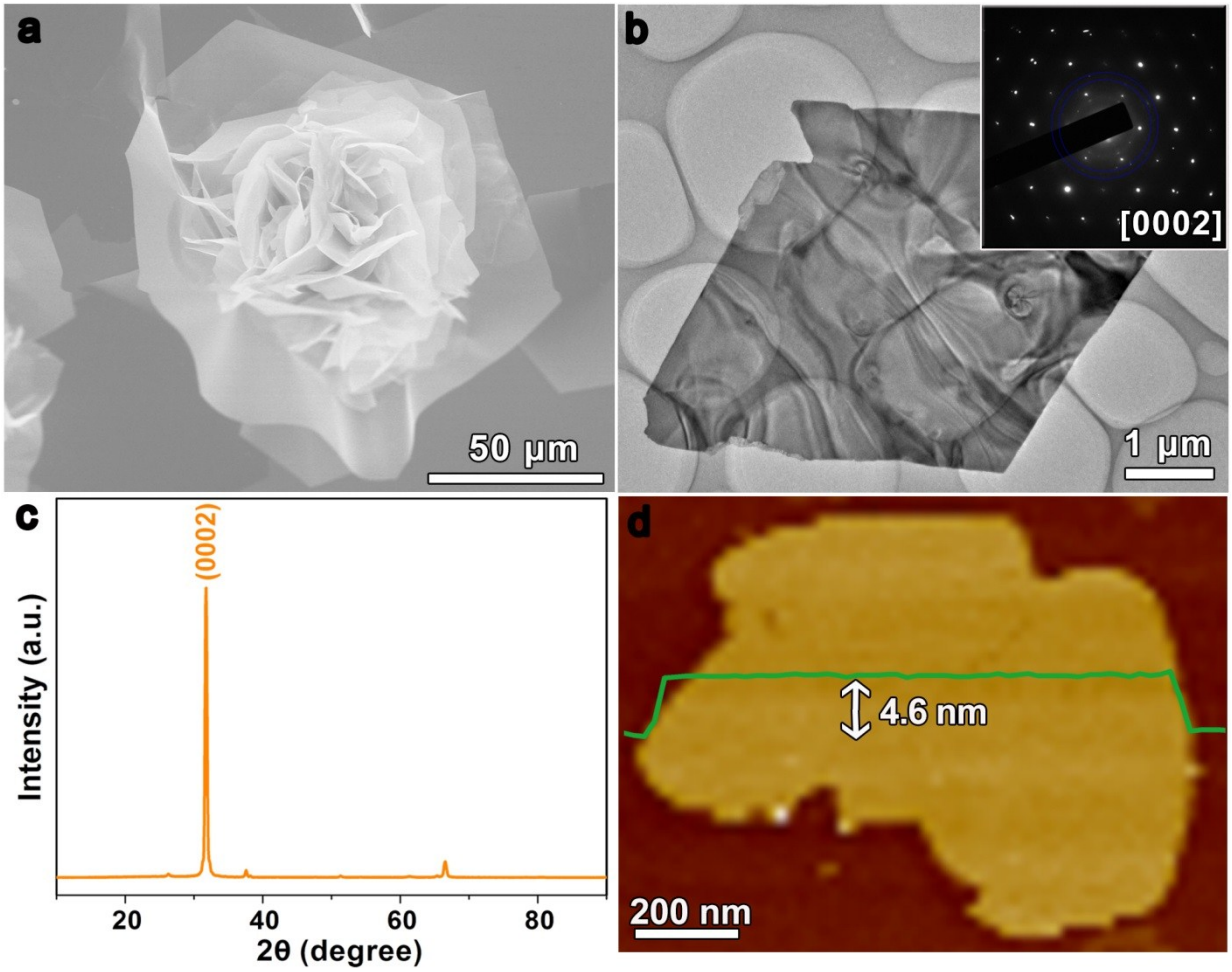

Figure S1. Characterizations of sulfide/metal/sulfide NSs. (a) Top-view SEM image. (b) TEM image and corresponding SAED pattern (inset). (c) XRD pattern of the product on FTO substrate. (d) AFM image and corresponding height profile.

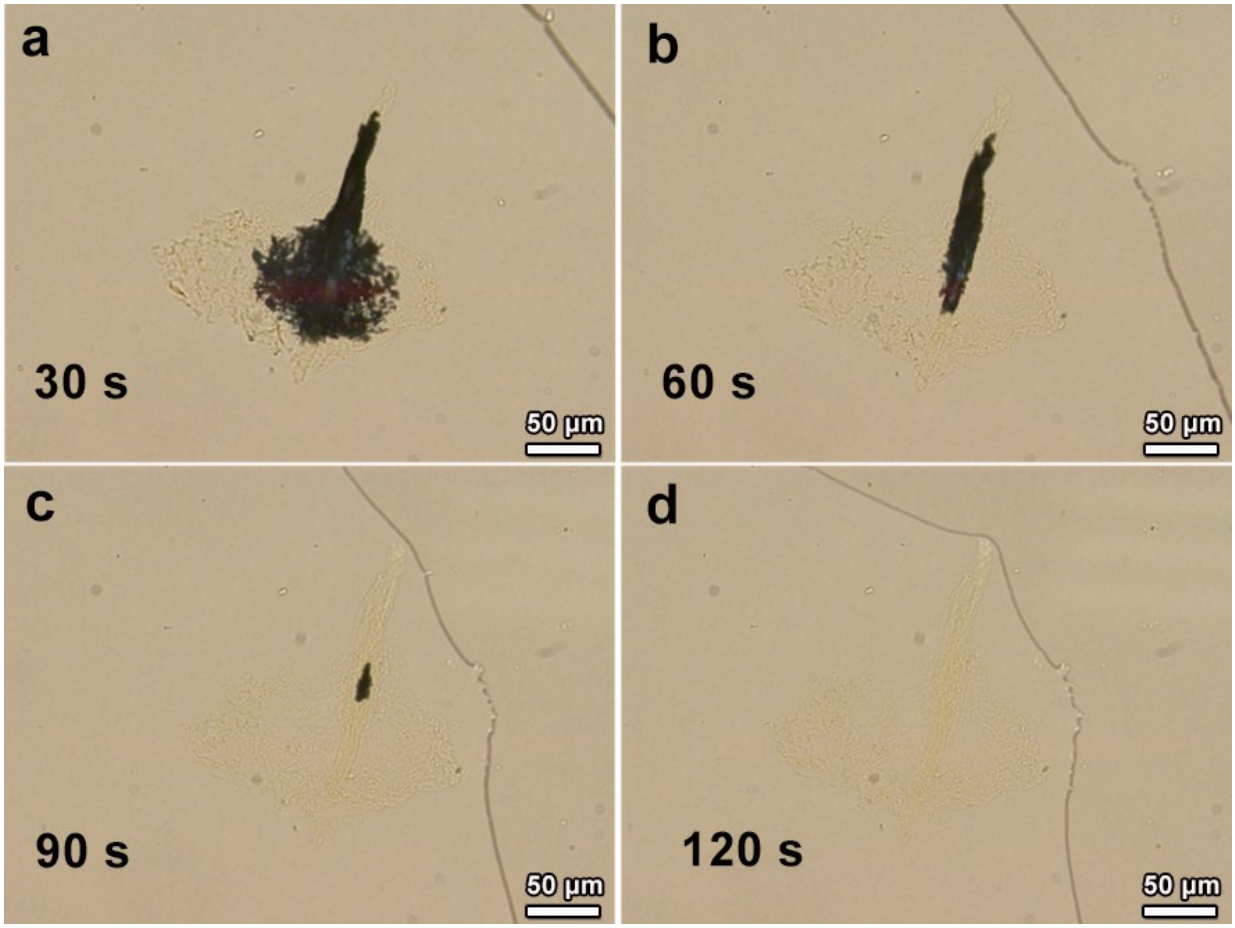

Figure S2. In-situ optical images of the etching process.

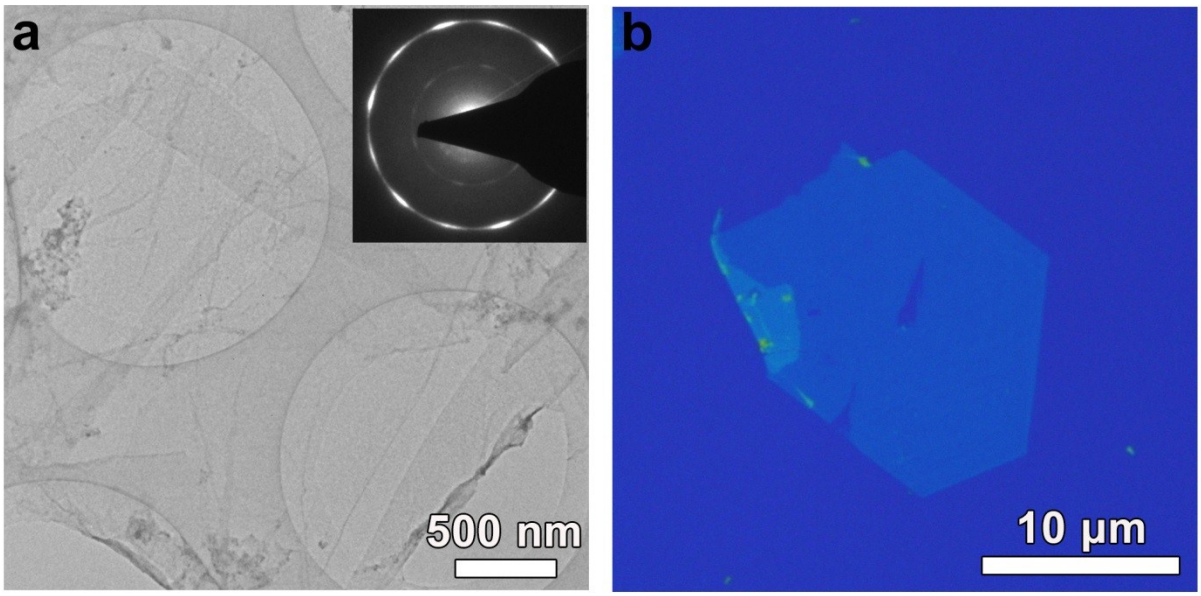

Figure S3. Characterizations of 1 nm NSs. (a) TEM image and corresponding SAED pattern (inset). (b) Optical image.

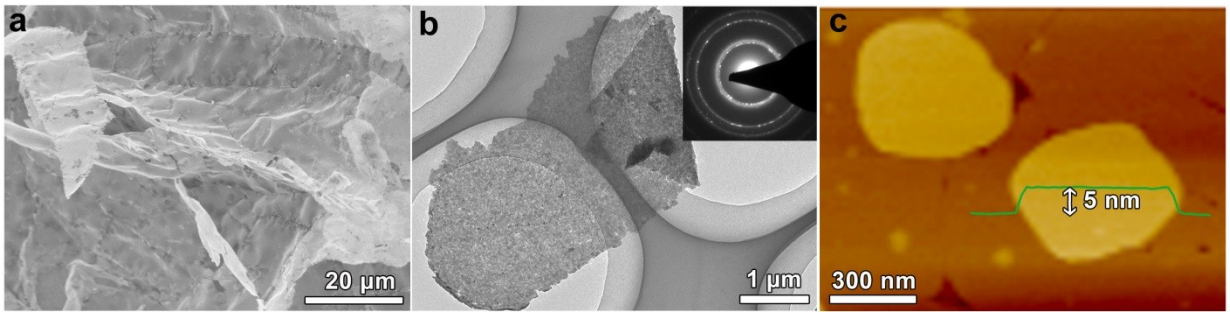

Figure S4. Characterization of 5 nm NSs. (a) SEM image, (b) TEM image, (c) AFM image.

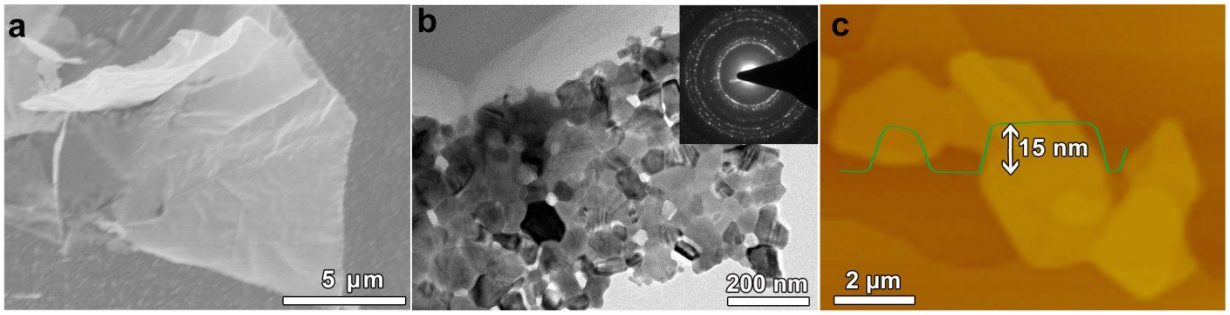

Figure S5. Characterization of 15 nm NSs (a) SEM image, (b) TEM image, (c) AFM image.

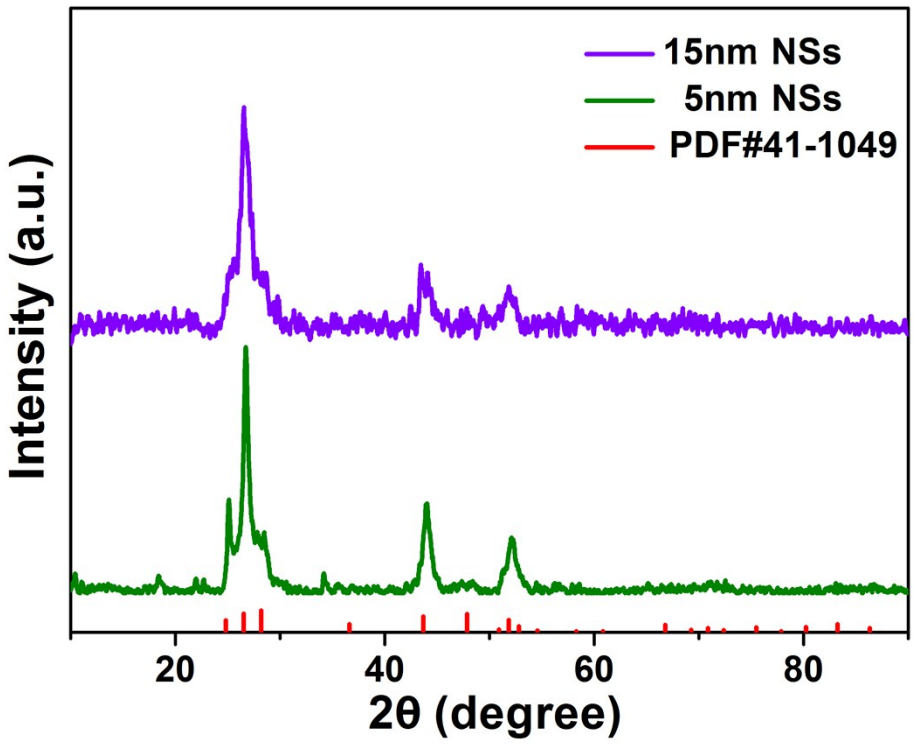

Figure S6. XRD spectra of as-fabricated CdS NSs with different thicknesses.

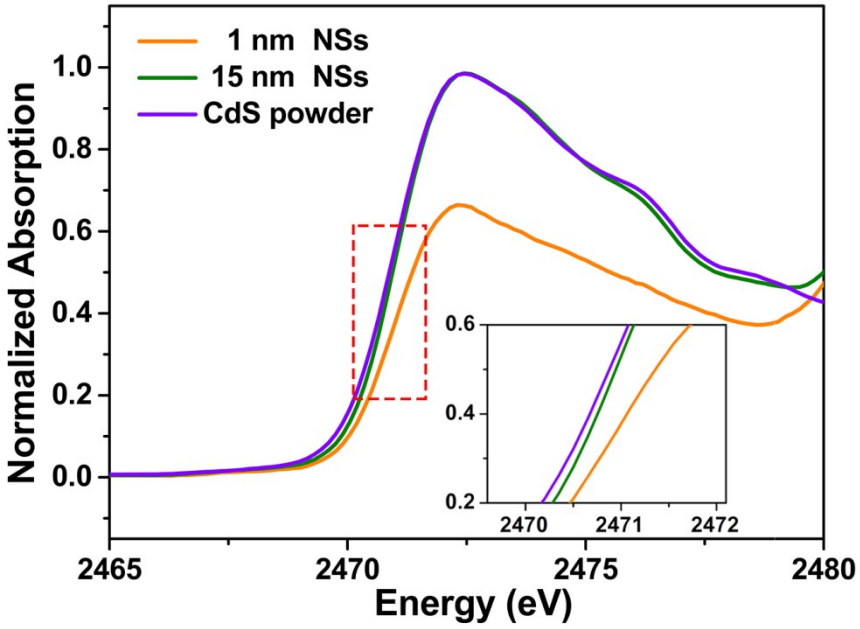

Figure S7. S K-edge XANES spectrum of CdS samples.

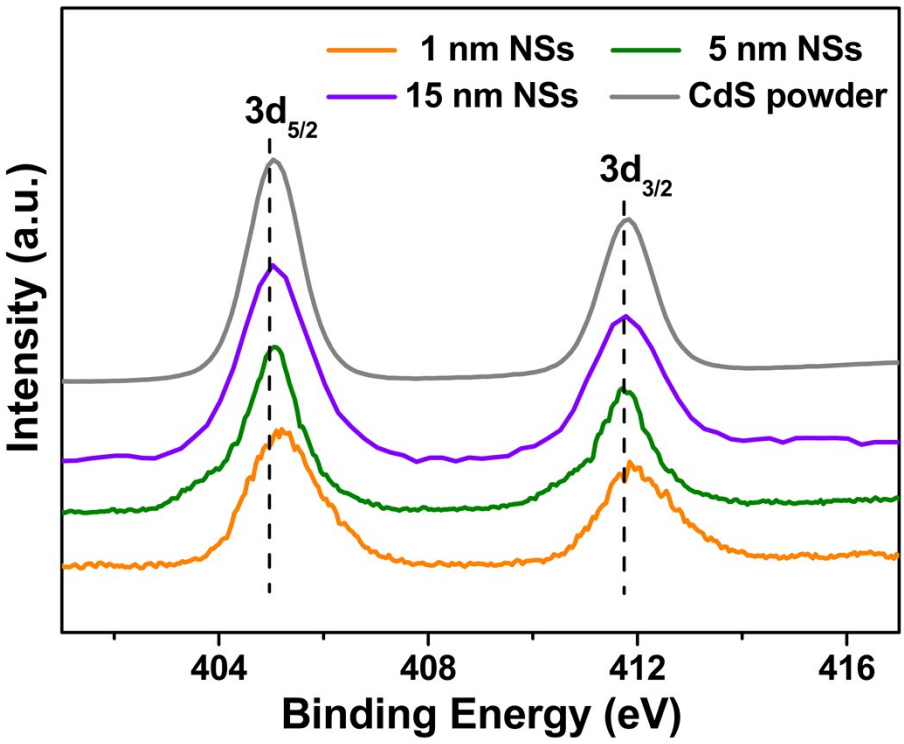

Figure S8. Cd 3d XPS spectrum of CdS samples.

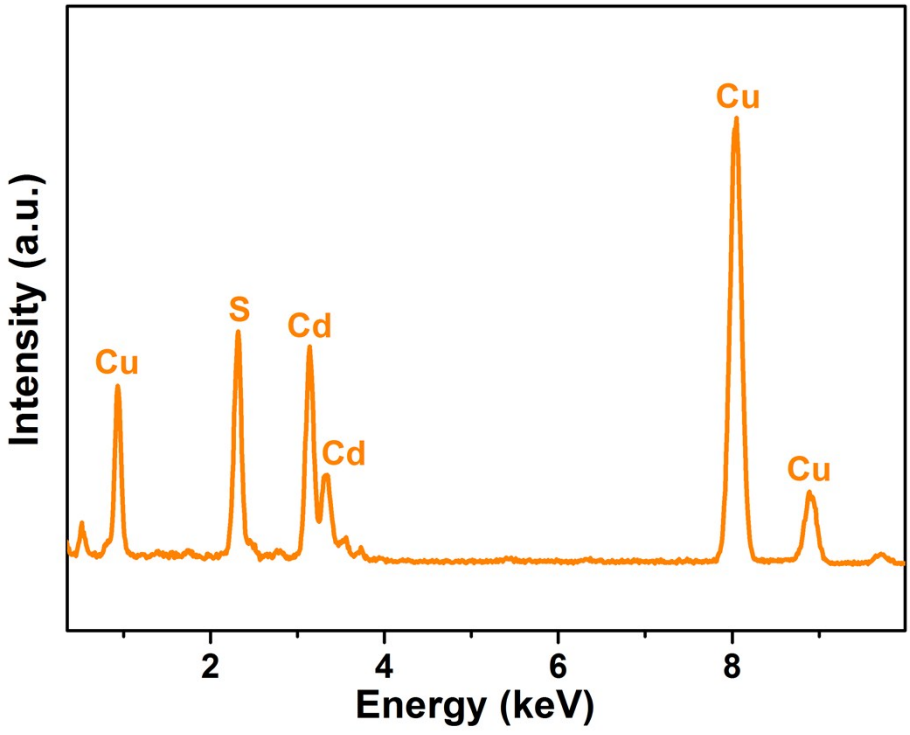

Figure S9. EDS spectrum of 1 nm NSs.

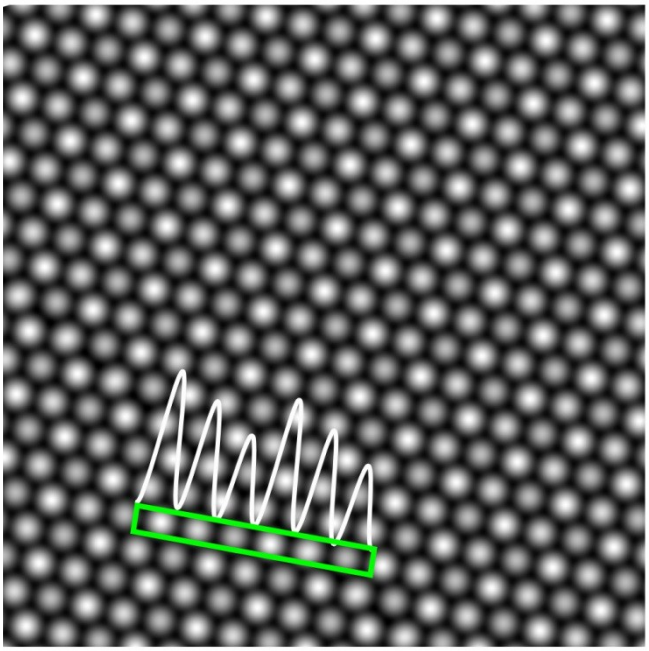

Figure S10. The simulated high-resolution STEM image of 1 nm NSs in Figure 2b and corresponding intensity profile.

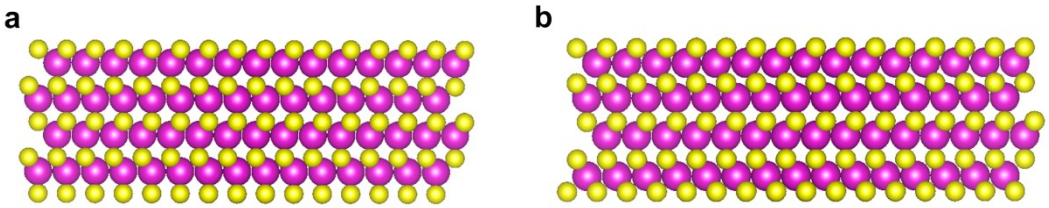

Figure S11. The crystal structures before (a) and after (b) the surface reconstruction.

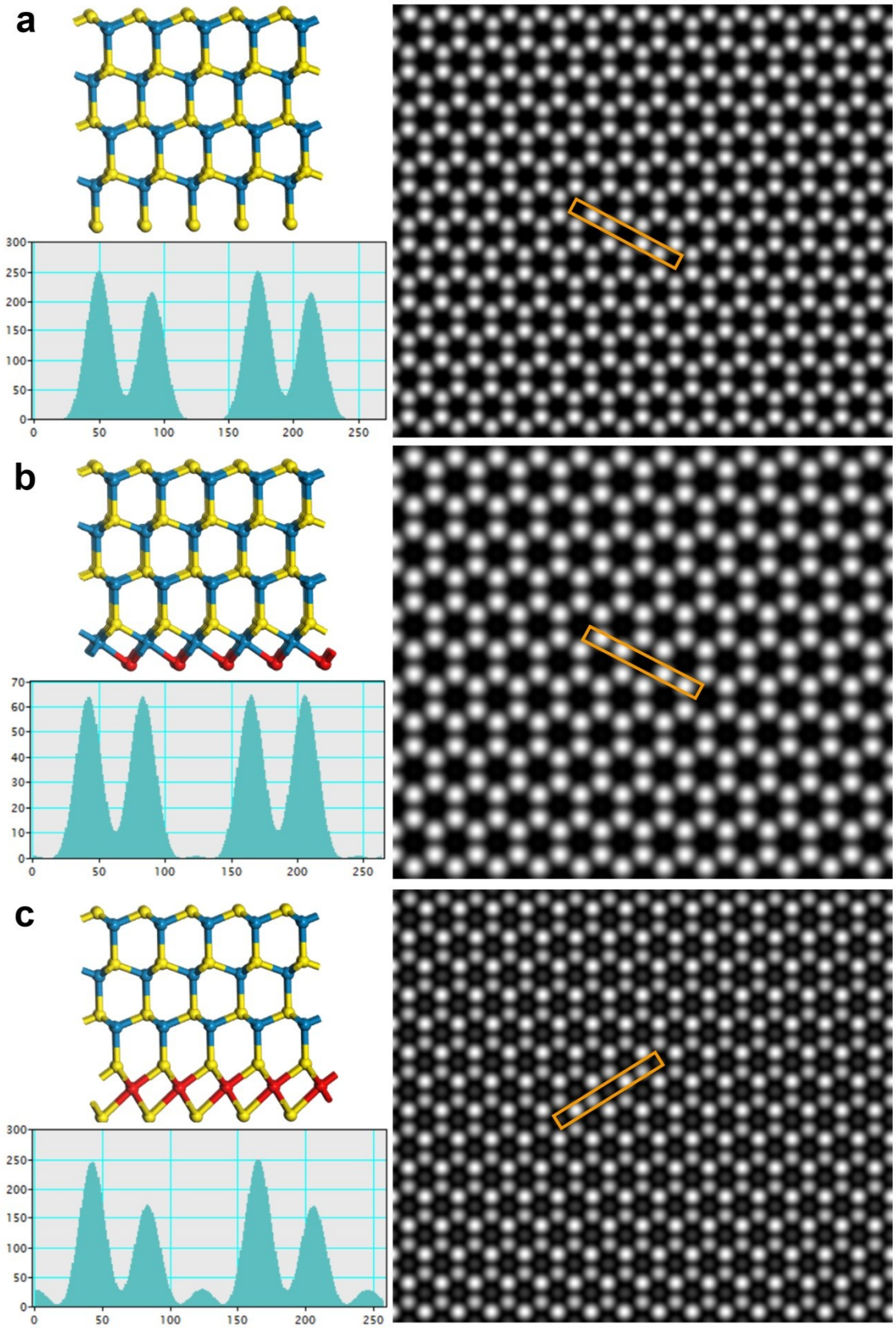

Figure S12. The crystal structures and corresponding simulation STEM images after the slip of single atomic layer in 1 nm NSs.

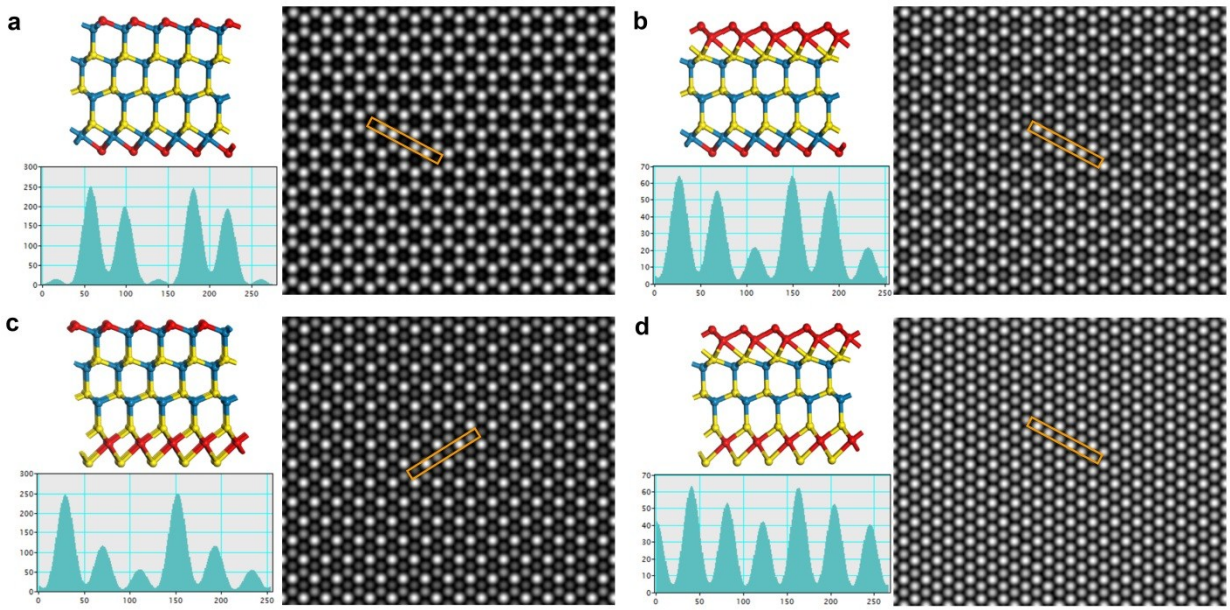

Figure S13. The crystal structures and corresponding simulation STEM images after the slip of both upper and lower atomic layer in 1 nm NSs.

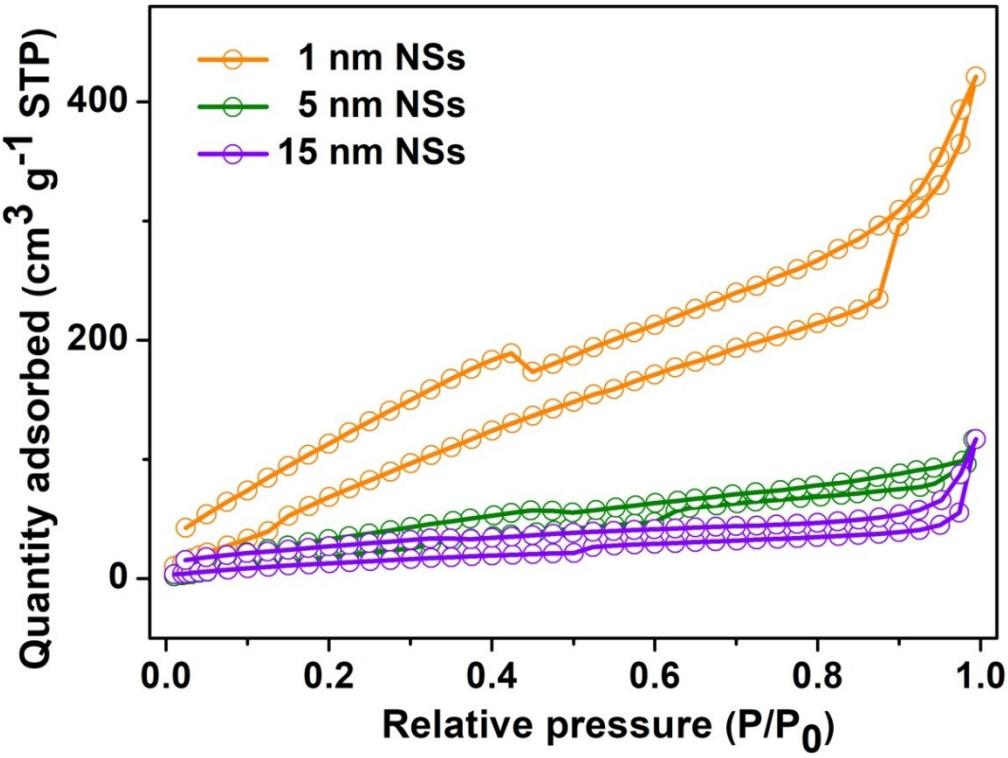

Figure S14. Nitrogen adsorption and desorption isotherms of 15 nm, 5 nm and 1 nm NSs.

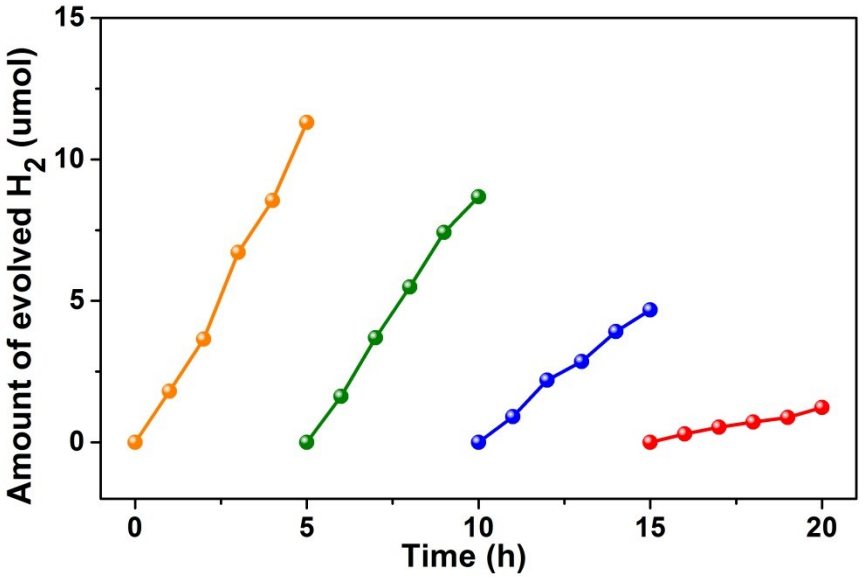

Figure S15. The stability of H_2 evolution of 5 nm NSs under visible light irradiation (>420 nm).

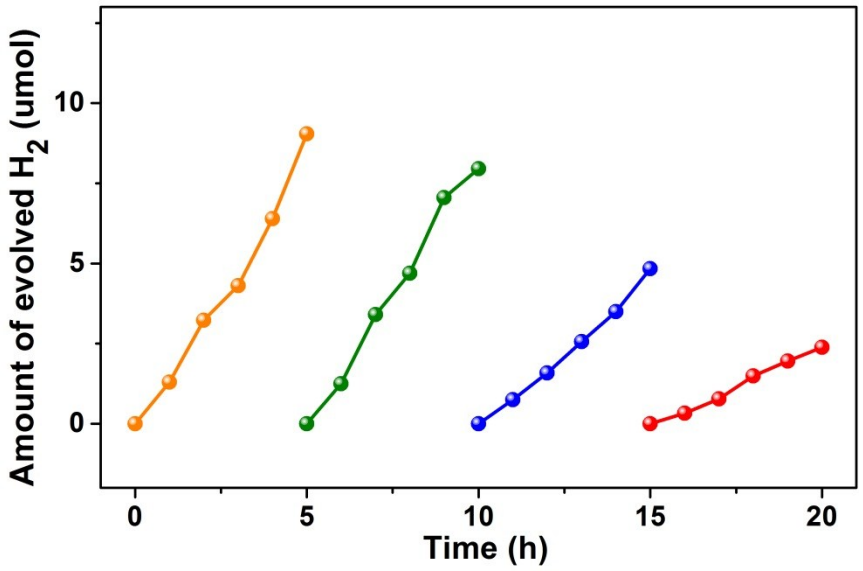

Figure S16. The stability of H_2 evolution of 15 nm NSs under visible light irradiation (>420 nm).

.

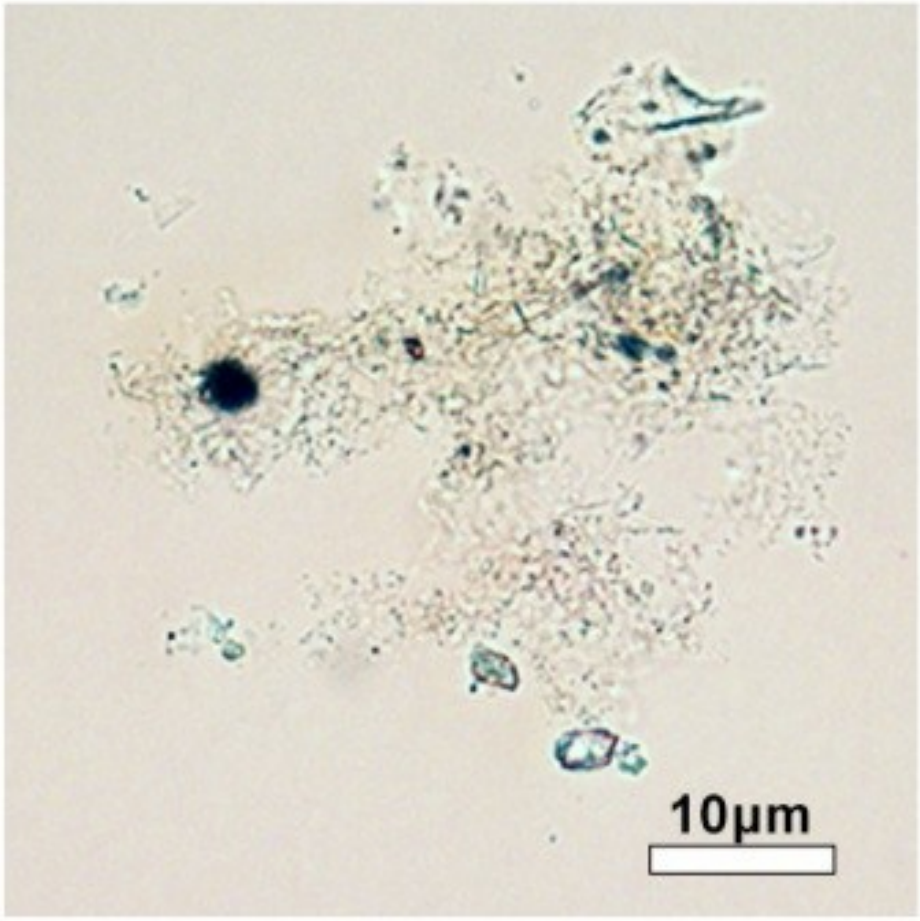

Figure S17. Optical image of 1 nm NSs after serving as catalysts for a 50 h H_2 evolution.

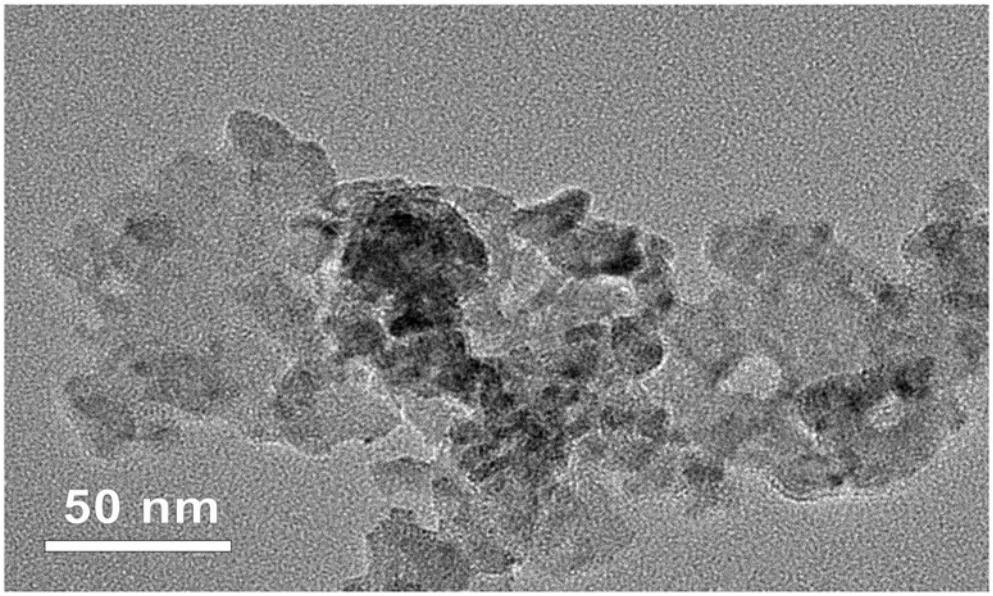

Figure S18. TEM image of 1 nm NSs after serving as catalysts for a 50 h H_2 evolution.

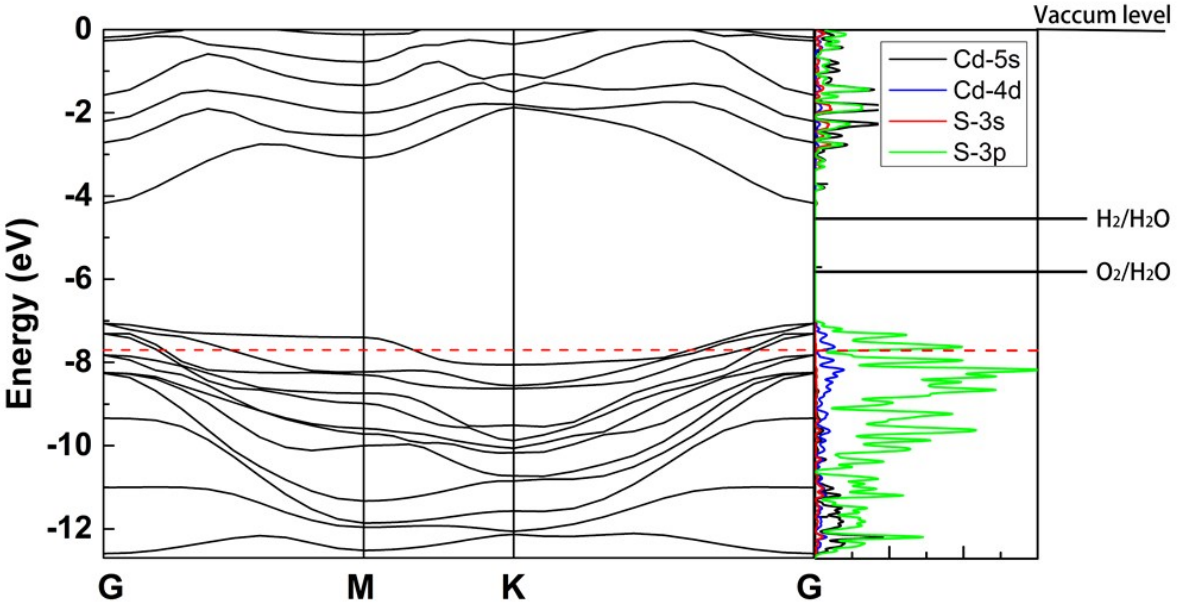

Figure S19. Calculated DOS of 1 nm NSs

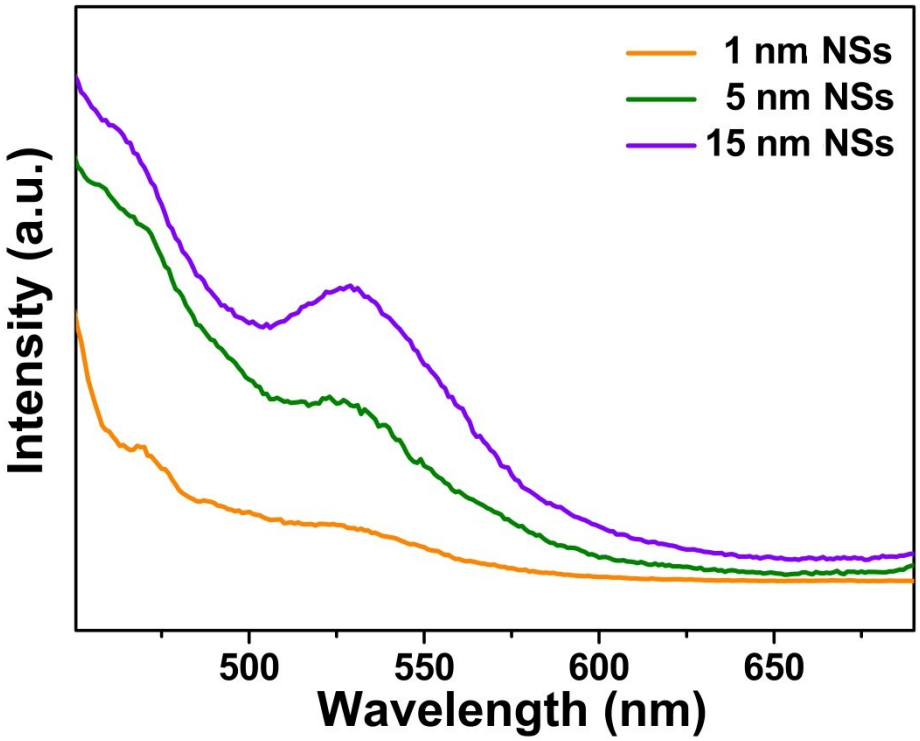

Figure S20. PL spectra of CdS NSs with different thickness.

3. Supplementary Tables

Table S1 Summary on the thickness and size of reported ultrathin CdS NSs.

photocatalyst	thickness	lateral size	synthetic method	references
1 nm NSs	1nm	10 μm	chemical vapor deposition	this work
CdS	4 nm	100 -300 nm	ultrasonic-induced aqueous exfoliation	[2]
CdS	2.16 nm	90 nm*20 nm	thermal decomposition	[3]
CdS	1.5 nm,	2.5 μm	oil bath	[4]

Table S2 The S/Cd atom ratio of 1 nm CdS NSs with different quantitative methods.

quantitative method	S/Cd atom ratio
XPS	1.226:1
EDS(from TEM)	1.362:1

Table S3 The calculated bader charge of 1 nm NSs.

bader charge	bulk CdS	1nm NSs
1S		-0.53834
2S		-0.76174
3S	-0.850922	-0.76957
4S		-0.62956
5S		-0.45645
1Cd		0.74814
2Cd		0.79754
3Cd	0.8509197	0.76884
4Cd		0.84837

Table S4 Summary on the photocatalytic properties of different CdS nanomaterials.

photocatalyst	Co-catalyst	sacrificial agent	Hydrogen production rate	quantum yield	Hydrogen evolution stability	references
1 nm NSs	no	ethanol	29.44 mmol/h/g (300 W xenon lamp, >420nm,)	AQY 4.15% IQY 55.65% (at 420nm)	50h remained 61.46%	this work
4 nm CdS nanosheets	no	Na_2S-Na_2SO_3	41.1 mmol/h/g (300 W xenon lamp, >420nm,)	AQY 1.38% (at 420nm)	12h	[3]
CdS–DETA nanosheets			7.5 mmol/h/g (300 W xenon lamp, >420nm,)	n.d.[a]		
2.16 nm CdS nanosheets	no	ethanol	n.d.	AQY 0.95% (at 405nm)	18h	[4]
1.5 nm CdS nanosheets	no	Na_2S-Na_2SO_3	2.155 mmol/h/g (350 W xenon lamp, >420nm,)	AQY 7.8% (at 420nm)	n.d.	[5]
CdS nanoparticles	phosphorene nanosheet	Lactic acid	11.192 mmol/h/g (300 W xenon lamp, >420nm,)	AQY 34.7% (at 420nm)	20h	[6]
CdS nanoparticles	WS_2	LA	14.10 mmol/h/g (300 W xenon lamp, >420nm,)	AQY 70% (at 465nm)	9h	[7]

CdS nanocrystals	MoS_2	Lactic acid	1.472 mmol/h/g (300 W xenon lamp, >420nm,)	n.d.	16h remained 70%	[7]
CdS nanoplates	no	Na_2S-Na_2SO_3	1.61 mmol/h/g (300 W xenon lamp, >420nm,)	n.d.	12h	[8]
	NiS	Na_2S-Na_2SO_3	22.3 mmol/h/g_{CdS} (300 W xenon lamp, >420nm,)	AQY 18% (at 425nm)	12h	
CdS nanoparticles	no	Na_2S-Na_2SO_3	8.31 mmol/h/g (300 W xenon lamp, >420nm,)	AQY 42% (at 425nm)	10h	[9]
Bulk CdS			1.73 mmol/h/g (300 W xenon lamp, >420nm,)	n.d.	n.d.	
CdS nanorods	no	Lactic acid	2.10 mmol/h/g (300 W xenon lamp, >400nm,)	n.d.	20h	[10]
	Pt		10.29 mmol/h/g (300 W xenon lamp, >400nm,)			
$Cd_{0.5}Zn_{0.5}S$	no	Na_2S-Na_2SO_3	25.8 mmol/h/g (300 W xenon lamp, >430nm,)	AQY 62% (at 425nm)	28h	[11]

[a] "n.d." represents "no data"

4. Supplementary References

1. X. H. Liu, P. F. Yin, S. A. Kulinich, Y. Z. Zhou, J. Mao, T. Ling, X. W. Du, ACS Appl Mater Interfaces. 2017, **9**, 602.

2. Yu. S, Fan. X. B, Wang. X, Li. J, Nat Commun, 2018, **9**, 4009.

3. Xu. Y, Zhao. W, Xu. R, Shi. Y, Zhang. B, Chem Commun (Camb). 2013, **49**, 9803.

4. Zhukovskyi. M, Tongying. P, Yashan. H, Wang. Y, Kuno. M, ACS Catalysis. 2015, **5**, 6615.

5. Bie. C, Fu. J, Cheng. B, Zhang. L, Applied Surface Science. 2018, **462**, 606.

6. Ran. J, Zhu. B, Qiao. S. Z, Angew Chem Int Ed Engl. 2017, **56**, 10373.

7. Chen. J, Wu. X. J, Yin. L, Li. B, Hong. X, Fan. Z, Angew Chem Int Ed Engl. 2015, **54**, 1210.

8. Wang. X, Liu. M, Zhou. Z, Guo. L, The Journal of Physical Chemistry C. 2015, **119**, 20555.

9. Yu. G, Geng. L, Wu. S, Yan. W, Liu. G, Chem Commun (Camb). 2015, **51**, 10676.

10. Zhang. L, Fu. X, Meng. S, Jiang. X, Wang. J, Chen. S, Journal of Materials Chemistry A. 2015, **3**, 23732.

11. Liu. M, Jing. D, Zhou. Z, Guo. L, Nat Commun. 2013, **4**, 2278.